Electronic Supplementary Material (ESI) for Soft Matter.

Supporting information for: "A multi-fluid model for microstructure formation in polymer membranes"

Douglas R. Tree,[†] Kris T. Delaney,[†] Hector D. Ceniceros,[‡] Tatsuhiro Iwama,[¶] and Glenn H. Fredrickson[*,§]

[†]*Materials Research Laboratory, University of California, Santa Barbara, CA 93106-5121*

[‡]*Department of Mathematics, University of California, Santa Barbara, CA 93106-5121*

[¶]*Asahi Kasei Corporation, 2-1 Samejima, Fuji, Shizuoka 416-8501 Japan*

[§]*Materials Research Laboratory, Materials Department and Chemical Engineering Department, University of California, Santa Barbara, CA 93106-5121*

E-mail: drt@mrl.ucsb.edu

Obtaining Transport Equations from the Rayleighian

In this section, we show how the Rayleighian specified in the main manuscript produces the transport equations in Equations 18–21. Substituting Equations 11, 12 and 17 into Eq. 6 gives the fully specified Rayleighian for the ternary multi-fluid model,

$$\begin{aligned} R[\{\boldsymbol{v}_i\}] = \int d\boldsymbol{r} \Bigg[\sum_i^{p,n,s} \frac{\zeta_i}{2} \left(\boldsymbol{v}_i - \boldsymbol{v}_m\right)^2 + \frac{1}{2} \boldsymbol{\sigma}^{(\mathrm{v})} : \nabla \boldsymbol{v} \\ - p \left(\nabla \cdot \boldsymbol{v}\right) + \sum_i^{p,n} \phi_i \boldsymbol{v}_i \cdot \nabla \mu_i \Bigg]. \end{aligned} \tag{1}$$

Component force balances are given by stationary values of the functional derivatives of the Rayleighian (*i.e.*, the Euler-Lagrange equations),

$$\frac{\delta R}{\delta \boldsymbol{v}_i} = \frac{\partial \mathcal{R}}{\partial \boldsymbol{v}_i} - \nabla \cdot \frac{\partial \mathcal{R}}{\partial \nabla \boldsymbol{v}_i} = 0 \tag{2}$$

where $\mathcal{R}$ is the integrand of the Rayleighian. Taking these functional derivatives and substituting Equations 4 and 14 to eliminate $\boldsymbol{v}$ and $\boldsymbol{v}_m$ yields,

$$\frac{\delta R}{\delta \boldsymbol{v}_p} = \frac{\zeta_p \zeta_n}{\zeta}(\boldsymbol{v}_p - \boldsymbol{v}_n) + \frac{\zeta_p \zeta_s}{\zeta}(\boldsymbol{v}_p - \boldsymbol{v}_s) - \phi_p \nabla \cdot \boldsymbol{\sigma}^{(\mathrm{v})} + \phi_p \nabla p + \phi_p \nabla \mu_p \tag{3}$$

$$\frac{\delta R}{\delta \boldsymbol{v}_n} = \frac{\zeta_p \zeta_n}{\zeta}(\boldsymbol{v}_n - \boldsymbol{v}_p) + \frac{\zeta_n \zeta_s}{\zeta}(\boldsymbol{v}_n - \boldsymbol{v}_s) - \phi_n \nabla \cdot \boldsymbol{\sigma}^{(\mathrm{v})} + \phi_n \nabla p + \phi_n \nabla \mu_n \tag{4}$$

$$\frac{\delta R}{\delta \boldsymbol{v}_s} = \frac{\zeta_p \zeta_s}{\zeta}(\boldsymbol{v}_s - \boldsymbol{v}_p) + \frac{\zeta_n \zeta_s}{\zeta}(\boldsymbol{v}_s - \boldsymbol{v}_n) - \phi_s \nabla \cdot \boldsymbol{\sigma}^{(\mathrm{v})} + \phi_s \nabla p. \tag{5}$$

The total momentum equation is readily obtained by summing Equations 3 through 5,

$$0 = -\nabla p + \nabla \cdot \boldsymbol{\sigma}^{(v)} - \sum_i^{p,n} \phi_i \nabla \mu_i. \tag{6}$$

This equation can be more compactly written by introducing the osmotic stress tensor,[S1–S4]

$$\nabla \cdot \boldsymbol{\Pi} = \sum_i^{p,n} \phi_i \nabla \mu_i \tag{7}$$

which gives

$$0 = -\nabla p + \nabla \cdot \boldsymbol{\sigma}^{(v)} - \nabla \cdot \boldsymbol{\Pi}. \tag{8}$$

Component diffusion equations can be obtained by combining Equations 3 through 5 with the conservation of mass expression in Eq. 2. We define the diffusive flux of component i as,

$$\boldsymbol{j}_i = \phi_i \left(\boldsymbol{v} - \boldsymbol{v}_i\right) \tag{9}$$

which allows us to re-write Eq. 2 as,

$$\frac{\partial \phi_i}{\partial t} + \boldsymbol{v} \cdot \nabla \phi_i = \nabla \cdot \boldsymbol{j}_i. \tag{10}$$

Substituting the definition of the friction coefficient from Eq. 15 into Equations 3–5 and using the definition of diffusive flux gives,

$$\boldsymbol{j}_p = \mathrm{v}_0 \zeta_0^{-1} \left[-\phi_p \nabla \cdot \boldsymbol{\sigma}^{(\mathrm{v})} + \phi_p \nabla p + \phi_p \nabla \mu_p \right] \tag{11}$$

$$\boldsymbol{j}_n = \mathrm{v}_0 \zeta_0^{-1} \left[-\phi_n \nabla \cdot \boldsymbol{\sigma}^{(\mathrm{v})} + \phi_n \nabla p + \phi_n \nabla \mu_n \right] \tag{12}$$

$$\boldsymbol{j}_s = -\mathrm{v}_0 \zeta_0^{-1} \left[\phi_s \nabla \cdot \boldsymbol{\sigma}^{(\mathrm{v})} + \phi_s \nabla p \right] \tag{13}$$

To isolate the diffusive flux, we eliminate the pressure terms from Equations 11–13 by performing the operations,

$$\boldsymbol{j}_p(\phi_n + \phi_s) - \phi_p(\boldsymbol{j}_n + \boldsymbol{j}_s) \tag{14}$$

$$\boldsymbol{j}_n(\phi_p + \phi_s) - \phi_n(\boldsymbol{j}_p + \boldsymbol{j}_s) \tag{15}$$

and use the fact that (i) $\sum_i^{p,n,s} \phi_i = 1$ and (ii) $\sum_i^{p,n,s} \boldsymbol{j}_i = 0$. With these manipulations, Eq. 10 becomes,

$$\frac{\partial \phi_p}{\partial t} + \boldsymbol{v} \cdot \nabla \phi_p = \frac{\mathrm{v}_0}{\zeta_0} \nabla \cdot \Bigg[\phi_p(1-\phi_p)\nabla \mu_p - \phi_p \phi_n \nabla \mu_n \Bigg] \tag{16}$$

$$\frac{\partial \phi_n}{\partial t} + \boldsymbol{v} \cdot \nabla \phi_n = \frac{\mathrm{v}_0}{\zeta_0} \nabla \cdot \Bigg[-\phi_p \phi_n \nabla \mu_p + \phi_n(1-\phi_n)\nabla \mu_n \Bigg] \tag{17}$$

which are more compactly written matrix notation as

$$\frac{\partial \phi_i}{\partial t} + \boldsymbol{v} \cdot \nabla \phi_i = \nabla \cdot \left(\sum_{j=1}^{p,n} M_{ij} \nabla \mu_j \right) \tag{18}$$

where we have introduced the component mobility matrix

$$M_{pp} = \frac{\mathrm{V}_0}{\zeta_0}\phi_p(1-\phi_p) \tag{19}$$

$$M_{pn} = M_{np} = -\frac{\mathrm{V}_0}{\zeta_0}\phi_p\phi_n \tag{20}$$

$$M_{nn} = \frac{\mathrm{V}_0}{\zeta_0}\phi_n(1-\phi_n). \tag{21}$$

The gradient of the chemical potential appears in both Equations 8 and 18. Taking the requisite functional derivatives per the definition in Eq. 10 yields,

$$\mu_i = \frac{k_B T}{\mathrm{V}_0}\left(\frac{\partial f_0}{\partial \phi_i} - \kappa_i \nabla^2 \phi_i\right) \tag{22}$$

where $\partial f_0/\partial \phi_i$ is the derivative of the homogeneous free energy in Eq. 8 with respect to volume fraction of component i. Taking the gradient and using the chain rule gives a chemical potential gradient with explicit volume fraction terms,

$$\nabla \mu_i = \frac{k_B T}{\mathrm{V}_0}\sum_j^{p,n}\left[H_{ij}\nabla\phi_j - K_{ij}\nabla\nabla^2\phi_j\right] \tag{23}$$

where

$$H_{pp} = (N_p\phi_p)^{-1} + (N_s\phi_s)^{-1} - 2\chi_{ps} \tag{24}$$

$$H_{pn} = H_{np} = (N_s\phi_s)^{-1} + \chi_{pn} - \chi_{ns} - \chi_{ps} \tag{25}$$

$$H_{nn} = (N_n\phi_n)^{-1} + (N_s\phi_s)^{-1} - 2\chi_{ns} \tag{26}$$

is the Hessian matrix, and

$$K_{pp} = \kappa_p \tag{27}$$

$$K_{pn} = K_{np} = 0 \tag{28}$$

Table S1: Characteristic Scales

Scale	Expression	Description
R	$bN_r^{1/2}$	end-to-end distance of the reference polymer
τ	$N_r^2\eta_r \mathrm{v}_0/k_BT$	Rouse time of reference polymer
p^*	η_r/τ	viscous stress scale

$$K_{nn} = \kappa_n \tag{29}$$

is the matrix of gradient coefficients. Substituting Eq. 23 into Equations 8 and 18 gives,

$$-\nabla p + \nabla \cdot \boldsymbol{\sigma}^{(v)} = \frac{k_BT}{\mathrm{v}_0}\sum_{i,j}^{p,n} \phi_i \left(H_{ij}\nabla\phi_j - K_{ij}\nabla\nabla^2\phi_j\right) \tag{30}$$

$$\frac{\partial \phi_i}{\partial t} + \boldsymbol{v}\cdot\nabla\phi_i = \frac{k_BT}{\mathrm{v}_0}\nabla\cdot\left[\sum_{j,k}^{p,n} M_{ij}\left(H_{jk}\nabla\phi_k - K_{jk}\nabla\nabla^2\phi_k\right)\right]. \tag{31}$$

With a fully specified model, we seek to write Equations 30 and 31 in dimensionless form. We define the characteristic length scale to be

$$R = bN_r^{1/2} \tag{32}$$

the end-to-end distance of a reference polymer of length N_r. The characteristic time scale is set to the Rouse time in a solution with a reference viscosity η_r,

$$\tau = \frac{N_r^2\eta_r \mathrm{v}_0}{k_BT} \tag{33}$$

and the characteristic pressure scale is set to be

$$p^* = \eta_r/\tau. \tag{34}$$

These characteristic scales are summarized in Table S1.

Using the definitions of R, τ and p^*, the momentum equation from Eq. 30 becomes,

$$
\begin{aligned}
-\tilde{\nabla}\tilde{p} + \tilde{\nabla}\cdot\tilde{\boldsymbol{\sigma}}^{(v)} =& \frac{k_B T}{\mathrm{v}_0}\frac{\tau}{\eta_r}\sum_{i,j}^{p,n}\phi_i\left(H_{ij}\tilde{\nabla}\phi_j - K_{ij}R^{-2}\tilde{\nabla}\tilde{\nabla}^2\phi_j\right)\\
=& N_r\sum_{i,j}^{p,n}\phi_i\left[(N_r H_{ij})\tilde{\nabla}\phi_j - (N_r R^{-2}K_{ij})\tilde{\nabla}\tilde{\nabla}^2\phi_j\right]
\end{aligned}
\tag{35}
$$

where $\tilde{\nabla} = \nabla R$, $\tilde{p} = p/p^*$ and $\tilde{\boldsymbol{\sigma}}^{(v)} = \boldsymbol{\sigma}^{(v)}/p^*$. Similarly, the diffusion equation becomes,

$$
\begin{aligned}
\frac{\partial\phi_i}{\partial\tilde{t}} + \tilde{\boldsymbol{v}}\cdot\tilde{\nabla}\phi_i =& \frac{k_B T}{\mathrm{v}_0}\frac{\tau}{R^2}\tilde{\nabla}\cdot\left[\sum_{j,k}^{p,n}M_{ij}\left(H_{jk}\tilde{\nabla}\phi_k - R^{-2}K_{jk}\tilde{\nabla}\tilde{\nabla}^2\phi_k\right)\right]\\
=& \nabla\cdot\left\{\sum_{j,k}^{p,n}\left(\eta_r b^{-2}M_{ij}\right)\left[\left(N_r H_{jk}\right)\nabla\phi_k - \left(N_r R^{-2}K_{jk}\right)\nabla\nabla^2\phi_k\right]\right\}
\end{aligned}
\tag{36}
$$

where $\tilde{t} = t/\tau$, $\tilde{\boldsymbol{v}} = \boldsymbol{v}\tau/R$. The non-dimensionalization procedure suggests that we define a dimensionless gradient coefficient $\tilde{\kappa}_i = N_r R^{-2}\kappa_i$, a dimensionless mobility matrix $\tilde{M}_{ij} = \eta_r b^{-2}M_{ij}$ and a re-scaled Hessian matrix $\tilde{H}_{ij} = N_r H_{ij}$, which appear in Equations 22–24.

Finally, note that the Peclet number, which would normally appear before the diffusion term in Eq. 36 is equal to unity. This is a consequence of the fact that all of the convective flows in the system are internally generated. If there had been boundary conditions prescribing alternate length and time scales, it would have been possible to obtain $\mathrm{Pe} \neq 1$. However, the capillary number does appear in Eq. 35. Here there are two energy scales; surface energy is characterized by $k_B T$ and viscous energy by $\eta_r R^3/\tau$. This means that the capillary number

$$
\mathrm{Ca} = N_r^{-1} \tag{37}
$$

is fixed by the reference degree of polymerization and is a consequence of the way that the surface forces and viscous forces scale with the reference length scale. At the monomer length scale, $N_r = N_s \approx 1$ and $\mathrm{Ca} \approx 1$. However, zooming out to the scale of the polymer radius of gyration, $N_r = N_p$, $\mathrm{Ca} = N_p^{-1}$ and the surface tension forces are much stronger.

Ternary Phase Diagram

For fixed N_i and χ_{ij}, the homogeneous free energy in Eq. 8 can be used to produce a ternary phase diagram consisting of (i) a binodal, (ii) a spinodal and (iii) a critical point.

The binodal curve is typically obtained by equating the chemical potentials of each species in both phases. Because f_0 is an intrinsic quantity, it is convenient to use an equivalent formalism where we equate the exchange chemical potentials

$$\mu_i = \frac{\partial f_0}{\partial \phi_i} \tag{38}$$

and the osmotic pressure

$$\Pi = f_0 - \sum_i \phi_i \mu_i \tag{39}$$

in each phase.[S5] Substituting Eq. 8 into Equations 38 and 39 and assuming pseudo-binary parameters, gives

$$\frac{1}{N} \ln\left(\frac{\phi_p^\alpha}{\phi_p^\beta}\right) - \ln\left(\frac{1-\phi_p^\alpha-\phi_n^\alpha}{1-\phi_p^\beta-\phi_n^\beta}\right) + \chi\left(\phi_n^\alpha - \phi_n^\beta\right) = 0 \tag{40}$$

$$\ln\left(\frac{\phi_n^\alpha}{\phi_n^\beta}\right) - \ln\left(\frac{1-\phi_p^\alpha-\phi_n^\alpha}{1-\phi_p^\beta-\phi_n^\beta}\right) + \chi\left(\phi_p^\alpha - \phi_p^\beta\right) = 0 \tag{41}$$

$$\ln\left(\frac{1-\phi_p^\alpha-\phi_n^\alpha}{1-\phi_p^\beta-\phi_n^\beta}\right) + \left(\phi_p^\alpha - \phi_p^\beta\right)\left(1 - \frac{1}{N}\right) - \chi\left(\phi_p^\alpha\phi_n^\alpha - \phi_p^\beta\phi_n^\beta\right) = 0 \tag{42}$$

With four unknowns (ϕ_p^α, ϕ_n^α, ϕ_p^β, ϕ_n^β), these three equations define the binodal curve in composition space for a given χ and N.

The spinodal is calculated by setting the determinant of the Hessian matrix in Eq. 23 to zero,

$$Z \equiv \begin{vmatrix} H_{pp} & H_{nn} \\ H_{pn} & H_{np} \end{vmatrix} = 0 \tag{43}$$

and the critical point is given when both Eq. 43 and

$$\begin{vmatrix} \dfrac{\partial Z}{\partial \phi_p} & H_{nn} \\ \dfrac{\partial Z}{\partial \phi_n} & H_{np} \end{vmatrix} = 0 \tag{44}$$

are satisfied.[S6–S8] Both equations are straightforward to generate, but too long to conveniently reproduce here.

Without further approximation, the solution to all three equations require numerical methods. For this paper, we compute the phase diagram using a custom code in Python. We find the critical point by simultaneously solving Equations 43 and 44. We then solve Eq. 43 from $\phi_s = 0$ to the critical point, resolving the two branches of the spinodal. Finally, we compute the two branches of the binodals by first computing the phase co-existence point for a binary system ($\phi_s = 0$), and then solve Eq. 40- 42 marching ϕ_p^α from the polymer-rich solution of the binary problem to the critical point. Unlike Yilmaz and McHugh,[S7] we did not need to resort to a least-squares method to avoid the trivial solution. Rather, we used scipy's `optimize.fsolve()` function with an analytical Jacobian and a first-order continuation method to obtain initial guesses.

Theory of a 1D interface

The concentration profiles for our model can be found by minimizing the interfacial free energy,

$$\gamma[\phi_p, \phi_n] = F[\phi_p, \phi_n] - \frac{k_B T}{V} \int d\boldsymbol{r}\, f_{eq}(\phi_p, \phi_n) \tag{45}$$

of a two phase system where the α-phase $\{\phi_p^\alpha, \phi_n^\alpha\}$ at the left boundary, $x = -\infty$, is in equilibrium with the β-phase $\{\phi_p^\beta, \phi_n^\beta\}$ at the right boundary, $x = \infty$. $F[\phi_p, \phi_n]$ is the free energy functional given in Eq. 7 and

$$f_{eq}(\phi_p, \phi_n) = f_0(\phi_p^\alpha, \phi_n^\alpha) + (\phi_p - \phi_p^\alpha)\mu_p(\phi_p^\alpha, \phi_n^\alpha) + (\phi_n - \phi_n^\alpha)\mu_n(\phi_p^\alpha, \phi_n^\alpha) \tag{46}$$

is the equilibrium free energy absent any interfaces. Note that the choice of the α-phase for Eq. 46 is arbitrary and the μ_i that appear are the exchange chemical potentials.

There are two barriers to obtaining analytical results for the interfacial profiles described by Eq. 45. The first is that $\gamma[\phi_p, \phi_n]$ describes the profiles of both $\phi_p(\boldsymbol{r})$ and $\phi_n(\boldsymbol{r})$, requiring a simultaneous solution to two Euler-Lagrange equations. To avoid this, we assume that the solvent concentration is constant, $\phi_s \approx \bar{\phi}_s$, making the model truly binary ($\phi = \phi_p$, $\phi_n = 1 - \phi - \bar{\phi}_s$). In general, the solvent concentration is not truly constant between both phases, since the solvent may partition unequally as well as concentrate at the polymer/non-solvent interface. However, this effect is small enough to neglect in the strong segregation limit, which we justify below.

Assuming a binary system, and using the notation for the pseudo-binary parameters given above, we re-write Eq. 45 for a 1D interface as,

$$\gamma[\phi] = \frac{k_B T}{b^2} \int \frac{dx}{b} \left[\Delta f(\phi) + K(\dot{\phi})\right] \tag{47}$$

where

$$\Delta f(\phi) = f_0(\phi) - f_0(\phi^\alpha) - (\phi - \phi^\alpha)\mu(\phi^\alpha) \tag{48}$$

$$K(\dot{\phi}) = \kappa\, \dot{\phi}^2 \tag{49}$$

and

$$f_0(\phi) = \frac{\phi}{N}\ln\phi + \left(1 - \phi - \bar{\phi}_s\right)\ln\left(1 - \phi - \bar{\phi}_s\right) + \bar{\phi}_s \ln\bar{\phi}_s + \chi\phi\left(1 - \phi - \bar{\phi}_s\right) \tag{50}$$

with $\mu = \partial f_0/\partial\phi$. Eq. 47 has a Lagrangian form, which immediately implies that

$$\dot{\phi}(x) = \left[\frac{\Delta f(\phi)}{\kappa}\right]^{1/2} \tag{51}$$

The second barrier to progress is the appearance of logarithmic terms in Eq. 50. To surmount this barrier, we assume that the phases are strongly segregated ($\chi \gg 1$ and $N \gg 1$) and use perturbation theory.[S5] Expanding $f_0(\phi)$ in this limit allows us to find the equilibrium concentrations, ϕ_α and ϕ_β. Equating exchange chemical potentials, $\mu_\alpha = \mu_\beta$, and osmotic pressures, $\Pi_\alpha = \Pi_\beta$, for the pseudo-binary model in both phases gives,

$$\frac{1}{\chi N}\ln\left(\frac{\varphi^\alpha}{\varphi^\beta}\right) - \frac{1}{\chi}\ln\left(\frac{1-\varphi^\alpha}{1-\varphi^\beta}\right) - 2\left(1-\bar{\phi}_s\right)\left(\varphi^\alpha - \varphi^\beta\right) = 0 \tag{52}$$

$$\frac{1}{\chi}\ln\left(\frac{1-\varphi^\alpha}{1-\varphi^\beta}\right) + \left(\varphi^\alpha - \varphi^\beta\right)\left(\frac{1}{\chi} - \frac{1}{\chi N}\right) + \left(1-\bar{\phi}_s\right)\left[(\varphi^\alpha)^2 - (\varphi^\beta)^2\right] = 0 \tag{53}$$

where we have introduced the reduced volume fraction

$$\varphi^\nu = \phi^\nu/\left(1-\bar{\phi}_s\right) \tag{54}$$

such that $\varphi \in [0,1]$ for $\nu \in [\alpha,\beta]$.

Assuming that $\varphi^\alpha \approx \epsilon^\alpha$ and $\varphi^\beta \approx 1-\epsilon^\beta$, Eq. 52 and Eq. 53 reduce to,

$$\frac{1}{\chi N}\left(\ln\epsilon^\alpha + \epsilon^\beta\right) + \frac{1}{\chi}\left(\epsilon^\alpha + \ln\epsilon^\beta\right) - 2\left(1-\bar{\phi}_s\right)\left(\epsilon^\alpha + \epsilon^\beta - 1\right) = 0 \tag{55}$$

$$-\frac{1}{\chi}\left(\epsilon^\alpha + \ln\epsilon^\beta\right) + \left(\epsilon^\alpha + \epsilon^\beta - 1\right)\left(\frac{1}{\chi} - \frac{1}{\chi N}\right) + \left(1-\bar{\phi}_s\right)\left[(\epsilon^\alpha)^2 - (1-\epsilon^\beta)^2\right] = 0 \tag{56}$$

where we have used the Taylor expansion $\ln(1-\epsilon) \approx -\epsilon$ when appropriate. The largest term in Eq. 55–56 are of $\mathrm{O}(\ln\epsilon)$, so we can neglect terms of $\mathrm{O}(\epsilon)$. Doing so and re-arranging gives,

$$\epsilon^{\alpha} = \exp\left[-\chi N(1-\bar{\phi}_s)\right] \tag{57}$$

$$\epsilon^{\beta} = \exp\left[-\chi(1-\bar{\phi}_s)\right] \tag{58}$$

to leading order when $\chi \gg 1$ and $N \gg 1$. It can be shown using a similar perturbation expansion of the phase equilibrium equations for the full ternary model, that the solvent concentration is constant at $\mathrm{O}(\ln \epsilon)$, justifying the pseudo-binary assumption.

Fully solving Eq. 51 for the interfacial profile requires numerical methods, but, we can obtain an expression for the interfacial width regardless. A characteristic interfacial width can be defined as,[S5,S9]

$$l = \frac{\phi^{\beta} - \phi^{\alpha}}{\dot{\phi}(x=0)} \tag{59}$$

where we can substitute the right hand side of Eq. 51 for $\dot{\phi}$. Doing so requires an expression for Δf_0, which can be obtained by combining Eq. 48 and Eq. 50,

$$\Delta f_0(\phi) = \frac{\phi}{N}\ln\left(\frac{\phi}{\phi^{\alpha}}\right) + (1-\phi-\bar{\phi}_s)\ln\left(\frac{1-\phi-\bar{\phi}_s}{1-\phi^{\alpha}-\bar{\phi}_s}\right) \\ + \left(1-\frac{1}{N}\right)(\phi-\phi^{\alpha}) - \chi\left(\phi-\phi^{\alpha}\right)^2 \tag{60}$$

Assuming that $\varphi = 1/2$ at $x = 0$, and using the binodal curves described by Equations 57 and 58 gives the width in Eq. 52, where terms smaller than $\mathrm{O}(\frac{1}{\chi})$ and $\mathrm{O}(\frac{1}{\chi N})$ have been neglected.

Linear Stability Analysis

We begin by neglecting hydrodynamics (set $\boldsymbol{v} = 0$ everywhere) and linearizing Eq. 18 about the homogeneous state $\{\bar{\phi}_p, \bar{\phi}_n\}$,

$$\frac{\partial}{\partial t}\delta\phi_i = \sum_{j,k} \bar{M}_{ij}\left(\bar{H}_{jk}\nabla^2\delta\phi_k - K_{jk}\nabla^4\delta\phi_k\right) \tag{61}$$

where $\delta\phi_i = \phi_i - \bar{\phi}_i$, and $\bar{M}_{ij}$ and $\bar{H}_{jk}$ indicate constant matrices evaluated at $\bar{\phi}_p$ and $\bar{\phi}_n$. Taking the Fourier transform gives,

$$\frac{\partial}{\partial t}\delta\hat{\phi}_i = \sum_{j,k}\left(-\bar{M}_{ij}\bar{H}_{jk}\,q^2 - \bar{M}_{ij}K_{jk}\,q^4\right)\delta\hat{\phi}_k \tag{62}$$

which is useful, since the derivative operators can be simply expressed in Fourier space. Eq. 62 is a system of linear, first order differential equations, which has a formal solution in Fourier-space of

$$\delta\hat{\phi}_i(q,t) = \sum_k \exp\left[A_{ik}(q)t\right]\delta\hat{\phi}_k(q,0) \tag{63}$$

where

$$A_{ik}(q) = -\sum_j\left(\bar{M}_{ij}\bar{H}_{jk}\,q^2 + \bar{M}_{ij}K_{jk}\,q^4\right) \tag{64}$$

From Eq. 63 it is clear that $\hat{\phi}(q,t)$ becomes unstable (thus precipitating spinodal decomposition) when $A_{ik}(q)$ is no longer negative definite. By definition, $A_{ik}(q)$ is non-negative definite when one eigenvalue is greater than or equal to zero for some value of q. This can be made explicit by using a similarity transform of A_{ik}, giving

$$\delta\hat{\phi}_i(q,t) = \sum_{j,k,l} X_{ij}\exp\left[\Lambda_{jk}t\right]X^{-1}_{kl}\delta\hat{\phi}_l(q,0) \tag{65}$$

where

$$\Lambda_{jk} = \begin{pmatrix} \lambda_+ & 0 \\ 0 & \lambda_- \end{pmatrix} \tag{66}$$

and X_{ij} are the eigenvalue and eigenvector matrices of $A_{ik}(q)$. Since $A_{ik}(q)$ is rank two, there is a simple formula for the eigenvalues

$$\lambda_\pm = \frac{\mathcal{T}}{2} \pm \frac{\left(\mathcal{T}^2 - 4\mathcal{D}\right)^{1/2}}{2} \tag{67}$$

where $\mathcal{T} = \mathrm{tr}[A_{ik}(q)]$ and $\mathcal{D} = \det[A_{ik}(q)]$. By inspection, $\mathcal{T}$ is always less than zero. Therefore, λ_+ can only be positive when $\mathcal{D} < 0$, making $\mathcal{D} = 0$ the stability criteria.

We can decompose this determinant into two terms: one that depends on the mobility and one that depends on the equilibrium parameters alone,

$$\det[A_{ik}(q)] = -\det(\bar{M}_{ij} q^2)\ \det(\bar{H}_{jk} + K_{jk}\, q^2) \tag{68}$$

It can be shown (and it is also physically intuitive) that the mobility matrix, $\bar{M}_{ij}$, is always positive definite, and therefore it is only necessary to consider

$$\det(\bar{H}_{jk} + K_{jk}\, q^2) = 0 \tag{69}$$

for the stability analysis. This is re-assuring, since kinetics should not determine thermodynamic stability.

Re-writing Eq. 69,

$$\begin{vmatrix} \bar{H}_{pp} + \kappa_p q^2 & \bar{H}_{pn} \\ \bar{H}_{np} & \bar{H}_{nn} + \kappa_p q^2 \end{vmatrix} = 0 \tag{70}$$

highlights its relationship with Eq. 43, proving that the preceding analysis generates the spinodal curve when κ_p and κ_n are zero. When κ_p and κ_n are non-zero, a finite size system is stabilized by the gradient free energy until a critical wavelength, $2\pi/q_c$, above which the system becomes unstable. The critical wavenumber is given by solving Eq. 70, which is a bi-quadratic equation in q. Using the quadratic equation yields,

$$q_c^2 = -\left(\frac{\bar{H}_{pp}}{2\kappa_p} + \frac{\bar{H}_{nn}}{2\kappa_n}\right) \pm \left[\left(\frac{\bar{H}_{pp}}{2\kappa_p} - \frac{\bar{H}_{nn}}{2\kappa_n}\right)^2 + 4\frac{\bar{H}_{pn}}{2\kappa_p}\frac{\bar{H}_{np}}{2\kappa_n}\right]^{1/2}. \tag{71}$$

Once unstable, the spinodal decomposition is dominated by the fastest growing mode, q_m, which is the mode that maximizes $\lambda_+(q)$. Using its definition in Eq. 67 and the definition of the diffusivity matrix (D_{ij}) and the gradient matrix (B_{ij}) in Equations 56 and 28, we can get an expression for λ_+ in terms of D_{ij} and B_{ij},

$$\lambda_+ = -\frac{q^2}{2}\left[(D_{pp} + D_{nn}) + (B_{pp} + B_{nn})q^2\right] \tag{72}$$

$$+\, q^2\Big[\left\{(D_{pp} - D_{nn}) + (B_{pp} - B_{nn})q^2\right\}^2 \tag{73}$$

$$+\, 4(D_{pn} + B_{pn}q^2)(D_{np} + B_{np}q^2)\Big]^{1/2} \tag{74}$$

The fastest growing mode can be found by solving

$$\left.\frac{d\lambda_+}{dq}\right|_{q=q_m} = 0 \tag{75}$$

Unfortunately, there is no convenient closed-form expression for q_m for general parameters, like there is for q_c. However, Eq. 75 can be re-written in a more convenient form for numerical root-finding

$$\lambda_+\frac{d\mathcal{T}}{dq} - \frac{d\mathcal{D}}{dq} = 0 \tag{76}$$

which is valid so long as $\mathcal{T}^2 \neq 4\mathcal{D}$. Additionally, if we assume that the mobility and gradient matrices are scalars ($M_{ij} = M\delta_{ij}$ and $K_{ij} = \kappa\delta_{ij}$), then Eq. 72 is greatly simplified. In this case the fastest growing mode becomes,

$$q_m^2 = \frac{q_c^2}{2} \tag{77}$$

which is equivalent to the relation between q_m and q_c for binary systems.[S10]

Finally, note that in addition to q_m, one also obtains the rate of spinodal decomposition from the preceding analysis. The rate is given by

$$\lambda_m \equiv \lambda_+(q_m) \tag{78}$$

and has units of inverse time. For the case of scalar mobility and gradient matrices, one obtains the simple expression

$$\lambda_m = M\kappa q_m^4 \tag{79}$$

Dynamic scaling

To ensure that the coarsening exponent is not a simulation artifact, we verify in Figure S1 that the polymer structure factor, $S(q)$, and polymer density correlation function, $g(r)$, obey dynamic scaling at long times. Dynamic scaling requires the system to be self-similar, and therefore the structure factor and the density correlation function should both collapse to universal curves when scaled by some characteristic length, L. The structure factor has units of length squared and the correlation function is dimensionless, so $L^{-2}S(Lq)$ and $g(r/L)$ should be universal at long times.

Figure S1(a) shows that the structure factor for $\{\phi_p, \phi_n\} = \{0.3, 0.65\}$ (blue circles in Figures 6 and 7) scaled by $\langle q^{-1}\rangle$ for $t \geq 4096$ collapses to a universal curve. Figure S1(b) shows a similar collapse for the real-space correlation function, $g(r/R_g)$ where R_g is the location of the first zero of the unscaled $g(r)$. The inset to Figure S1(b) shows the product of R_g and $\langle q\rangle$, which approaches a steady value as $t \to \infty$. The latter plot demonstrates that because the system is self-similar, either $\langle q\rangle$ or R_g can be used as a characteristic length.

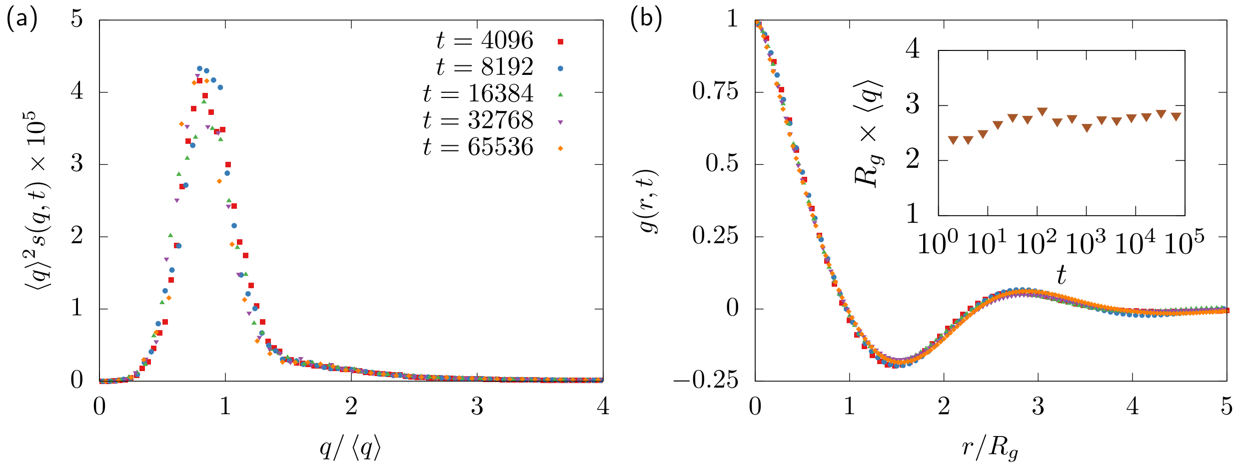

Figure S1: (a) Polymer structure factor versus wavevector, scaled by the first moment $\langle q\rangle$. (b) Polymer density correlation function versus radial distance, r, scaled by R_g, the first zero of $g(r)$. (inset to b) Product of R_g and $\langle q\rangle$ as a function of time, showing the equivalence of each measure of the domain size to within a constant value at long times. Data are from the one of the sets presented in Figures 6 and 7 (closed blue circles, diffusion only) with parameters: $N = 20$, $\chi = 0.973, \kappa = 2, \{\phi_p, \phi_n\} = \{0.3, 0.65\}$.

References

(S1) M. Doi and A. Onuki, *J. Phys. II France*, 1992, **2**, 1631–1656.

(S2) M. Cromer, M. C. Villet, G. H. Fredrickson, L. Gary Leal, R. Stepanyan and M. J. H. Bulters, *J. Rheol.*, 2013, **57**, 1211–1235.

(S3) S. T. Milner, *Phys. Rev. E*, 1993, **48**, 3674–3691.

(S4) H. Tanaka, *J. Phys.-Condens. Mat.*, 2000, **12**, R207.

(S5) D. Broseta, G. H. Fredrickson, E. Helfand and L. Leibler, *Macromolecules*, 1990, **23**, 132–139.

(S6) D. Broseta and G. H. Fredrickson, *J. Chem. Phys.*, 1990, **93**, 2927.

(S7) L. Yilmaz and A. J. McHugh, *J. Appl. Polym. Sci.*, 1986, **31**, 997–1018.

(S8) J. W. Gibbs, in *The Scientific Papers of J. Willard Gibbs. Vol 1. Thermodynamics*, Longmans, Green and Co., 1906, ch. On the Equilibrium of Heterogeneous Substances.

(S9) J. W. Cahn and J. E. Hilliard, *J. Chem. Phys.*, 1958, **28**, 258–267.

(S10) J. W. Cahn, *J. Chem. Phys.*, 1965, **42**, 93.